Kepler Stellar Properties Catalog Update for Q1-Q17 DR25 Transit Search

NASA Ames Research Center
Moffett Field, CA 94035

Prepared by: _____ Date __10/06/16__
Savita Mathur, Participating Scientist

Prepared by: _____ Date __10/06/16__
Daniel Huber, Participating Scientist

Approved by: _____ Date __10/06/16__
Michael R. Haas, Science Office Director

Approved by: _____ Date __10/06/16__
Natalie Batalha, Project Scientist

Document Control

Ownership

This document is part of the *Kepler* Project Documentation that is controlled by the *Kepler* Project Office, NASA/Ames Research Center, Moffett Field, California.

Control Level

This document will be controlled under KPO @ Ames Configuration Management system. Changes to this document **shall** be controlled.

Physical Location

The physical location of this document will be in the KPO @ Ames Data Center.

Distribution Requests

To be placed on the distribution list for additional revisions of this document, please address your request to the *Kepler* Science Office:

> Michael R. Haas
> *Kepler* Science Office Director
> MS 244-30
> NASA Ames Research Center
> Moffett Field, CA 94035-1000
>
> Michael.R.Haas@nasa.gov

DOCUMENT CHANGE LOG

CHANGE DATE	PAGES AFFECTED	CHANGES/NOTES
January 8, 2016	all	Original Release
April 15, 2016	16-21	Added section 3 on posteriors; renumbered subsequent sections
October 6, 2016	22	Added Section 4 on the new distances and extinctions

Table of Contents

1. Introduction

Huber et al. (2014) presented revised stellar properties for 196,468 *Kepler* targets, which were used for the Q1-Q16 TPS/DV planet search (Tenenbaum et al. 2014). The catalog was based on atmospheric properties (*i.e.*, temperature (T_{eff}), surface gravity (log(g)), and metallicity ([Fe/H])) published in the literature using a variety of methods (*e.g.*, astero-seismology, spectroscopy, exoplanet transits, photometry), which were then homogene-ously fitted to a grid of Dartmouth (DSEP) isochrones (Dotter et al. 2008). The catalog was updated in early 2015 for the Q1-Q17 DR24 transit search (Seader et al. 2015) based on the latest classifications of *Kepler* targets in the literature at that time. The methodolo-gy followed Huber et al. (2014).

Here we provide updated stellar properties of 197,096 *Kepler* targets. Like the previous catalog, this update is based on atmospheric properties that were either published in the literature or provided by the *Kepler* community follow-up program (CFOP). The input values again come from different methods: asteroseismology, spectroscopy, flicker, and photometry. This catalog update was developed to support the SOC 9.3 TPS/DV planet search (Twicken et al. 2016), which is expected to be the final search and data release by the *Kepler* project.

In this document, we describe the method and the inputs that were used to build the cata-log. The methodology follows Huber et al. (2014) with a few improvements as described in Section 2.

2.   Catalog Updates

2.1 Input Data

In this version of the catalog, we have included atmospheric properties that were recently published or acquired from ground-based follow-up of *Kepler* targets. The main new input values can be summarized as follows:

1) Two of the largest entries (>5,000 stars) come from publicly available spectroscopic surveys, namely LAMOST (medium resolution, R~1800) and APOGEE (high resolution, R~22,500).

2) For 14,535 stars we adopted surface gravities estimated from the detection of granulation in the *Kepler* data (*i.e.*, the Flicker method; Bastien et al. 2013, Bastien et al. 2015). We limited the applicability of the Flicker log(g) values to stars for which the reported uncertainty was smaller than 0.2 dex to ensure higher reliability for the input values.

3) For more than 1,000 stars, we used spectroscopic parameters provided by the *Kepler* community follow-up program (CFOP) that observed around 800 planet candidate hosts and 535 solar-like stars for which solar-like oscillations were detected in the *Kepler* data.

4) A sample of ~835 stars which were classified as dwarfs in the original *Kepler* Input Catalog (KIC) were shown to be red giants based on the detection of giant-like oscillations in the *Kepler* data. We adopted log(g) values estimated from asteroseismology in combination with revised effective temperatures for these stars (Mathur et al., in preparation).

5) For 62 newly confirmed *Kepler* exoplanet hosts we adopted stellar parameters as published in the discovery papers.

6) We also report spectroscopic parameters for 317 stars, which were so far unclassified but were included in either the APOGEE or LAMOST surveys. We added 310 stars that were first observed in Q17.
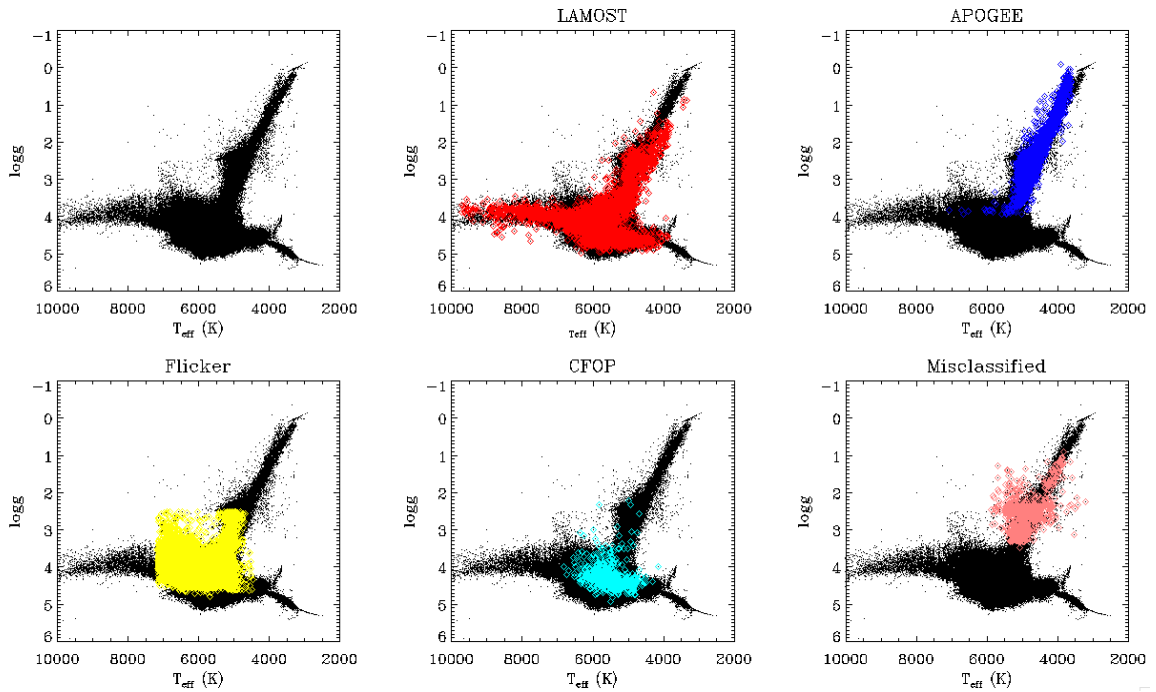
Figure 1: HR diagram showing the input values used for the final catalog with different panels for the big survey inputs.

Figure 1 shows the distribution of the largest new inputs from LAMOST, APOGEE, Flicker, CFOP, and the sample of misclassified red giants. Reference keys are listed in Table 1 for the input values added since the Q1-Q16 catalog (Huber et al. 2014).

These input values were prioritized as follows:

For surface gravity, the highest priority was given to asteroseismology, then high-resolution spectroscopy, low-resolution spectroscopy, flicker, photometric observations, and finally the KIC.

For temperature, the highest priority was given to high-resolution spectroscopy, followed by low-resolution spectroscopy, photometric observations, and the KIC. In other words, the priority was given to the CFOP observations and published values for confirmed planets, then APOGEE, LAMOST, and finally the KIC.

Table 1

Number of Stars	P_{Teff}	P_{logg}	$P_{[Fe/H]}$	$P_{M,R,rho}$	Reference
1784	PHO55	AST55	SPE55	DSEP	Pinsonneault et al. (2014)
969	PHO56	AST56	PHO56	DSEP	Casagrande et al. (2014)
130	SPE57	SPE57	SPE57	DSEP	Petigura et al. (2013)
143	SPE58	SPE58	SPE58	DSEP	Rowe et al. (2014)
315	SPE59	SPE59	SPE59	DSEP	Buchhave et al. (2014)
96	SPE60	SPE60	SPE60	DSEP	Mann et al. (2013a,b)
11	SPE61	SPE61	SPE61	DSEP	Marcy et al. (2014)
1	SPE62	SPE62	SPE62	DSEP	Borucki et al. (2013)
1	SPE63	SPE63	SPE63	DSEP	Sanchis-Ojeda et al. (2013)
1	SPE64	TRA64	SPE64	DSEP	Gandolfi et al. (2013)
1	SPE65	TRA65	SPE65	DSEP	Ofir et al. (2014)
1	SPE66	TRA66	SPE66	DSEP	Deleuil et al. (2014)
1	SPE67	SPE67	SPE67	DSEP	Tingley et al. (2014)
6383	SPE68	SPE68	SPE68	DSEP	Luo et al. (2015) (LAMOST)
32	SPE69	AST69	SPE69	DSEP	Silva Aguirre et al. (2015) (some stars T_{eff} and Fe/H were from previous papers)
90	SPE70	SPE70	SPE70	DSEP	Muirhead et al. (2014) (only one star with log(g) from SPE70, and one hot star with M and R from MULT70)
835	KIC0	AST71	KIC0	DSEP	Mathur et al. (in prep.)
535	SPE72	ASTX	SPE72	DSEP	Chaplin et al. (in prep.) (CFOP)
14535		FLK73		DSEP	Bastien et al. (2015)
5677	SPE74	SPE74	SPE74	DSEP	Alam et al. (2015) (APOGEE)
1	SPE75	SPE75	SPE75	DSEP	Mancini et al. (2015)
3	SPE76	SPE76	SPE76	DSEP	Almenara et al. (2015)
4	SPE77	SPE77	SPE77	DSEP	Hébrard et al. (2014)

Number of Stars	P_{Teff}	P_{logg}	$P_{[Fe/H]}$	$P_{M,R,rho}$	Reference
1	SPE78	SPE78	SPE78	DSEP	Santerne et al. (2014)
1	SPE79	SPE79	SPE79	DSEP	Dawson et al. (2014)
1	SPE80	SPE80	SPE80	DSEP	Kipping et al. (2014)
2	SPE81	SPE81	SPE81	DSEP	Endl et al. (2014)
1	SPE82	SPE82	SPE82	DSEP	Gandolfi et al. (2015)
1	SPE83	SPE83	KIC0	MULT83	Silvotti et al. (2014)
2	SPE84	SPE84	SPE84	DSEP	Everett et al. (2015)
8	SPE85	SPE85	SPE85	DSEP	Torres et al. (2015)
2	SPE86		SPE86	DSEP	Muirhead et al. (2015)
1	SPE87	SPE87	SPE87	DSEP	Lillo-Box et al. (2015)
1	SPE88	SPE88	SPE88	DSEP	Bourrier et al. (2015)
1	SPE89	SPE89	SPE89	DSEP	Borucki et al. (2012)
778	SPE90	SPE90	SPE90	DSEP	KOI CFOP

Table 1 contains a reference list key for the provenances added since the Q1-Q16 catalog. Columns 2 - 5 give the provenances for the designated input parameters, which are coupled to numbers denoting the references from which the input values were adopted. See Section 6.5 in Huber et al. (2014) for details.

2.2 Grid and Methodology

The input values (*i.e.*, T_{eff}, log(g), and [Fe/H]) were fitted to DSEP isochrones using typical uncertainties according to Table 2 of Huber et al. (2014) to derive interior properties. For the Flicker results, the adopted log(g) uncertainty is 0.2 dex.

We used the same Dartmouth grid as in Huber et al. (2014), with the exception of additional interpolation in mass for parameter spaces that were sparsely covered in the original grid. For stellar parameter inference we followed the Bayesian methodology described in Serenelli et al. (2013), which involves the direct integration of discrete likelihoods weighted by the volume that each model encompasses in mass, age and metallicity. We note that this method is equivalent to an MCMC, with the advantage that it is considerably faster, but the disadvantage that it does not automatically provide parameter correlations. The resulting Discrete posteriors were used to calculate one-sigma confidence intervals around the best-fit value for each parameter. Note that due to a coding error the

positions of the posteriors were accidentally shifted upwards by half of the integration step size for each parameter. This only affects the reported uncertainties and amounts to a small absolute shift (~1/20 sigma) for each parameter.

Figure 2 shows a few examples of Discrete posteriors for solar-type dwarfs with log(g) input values from asteroseismology, spectroscopy, and the KIC. In the asteroseismic case, the peak is very narrow compared to the other cases. The large input uncertainty in log(g) for the KIC yields a distribution which peaks at the main sequence (the most probable for a star with a weak log(g) constraint) and has a tail towards lower log(g) values. We note that the best-fit value does not always coincide with the mode of the posterior distribution. Adopting the best-fit was motivated by the fact that adopting the mode as a point estimate would lead to an unrealistically high number of main-sequence stars due to the fact that for a given input value of log(g) with a large uncertainty, a star will probabilistically be most likely on the main sequence. Since the *Kepler* target stars represent neither a volume nor a strictly magnitude-limited sample (see, for example, the target selection criteria as described in Batalha et al. 2010), constructing a prior to characterize the most probable evolutionary state of a *Kepler* target star is not straightforward. The stellar classification in the *Kepler* Input Catalog used a prior constructed from a volume-limited Hipparcos sample, which has been shown to underestimate the number of subgiants due to Malmquist bias (see, for example, Bastien et al. 2014). Adopting the best-fit values ensures that the point estimates reported in the catalog account for some of the expected Malmquist bias in the *Kepler* sample, but we caution that some systematic biases likely remain in the catalog (and these biases will likely not be fully resolved until Gaia parallaxes become available).
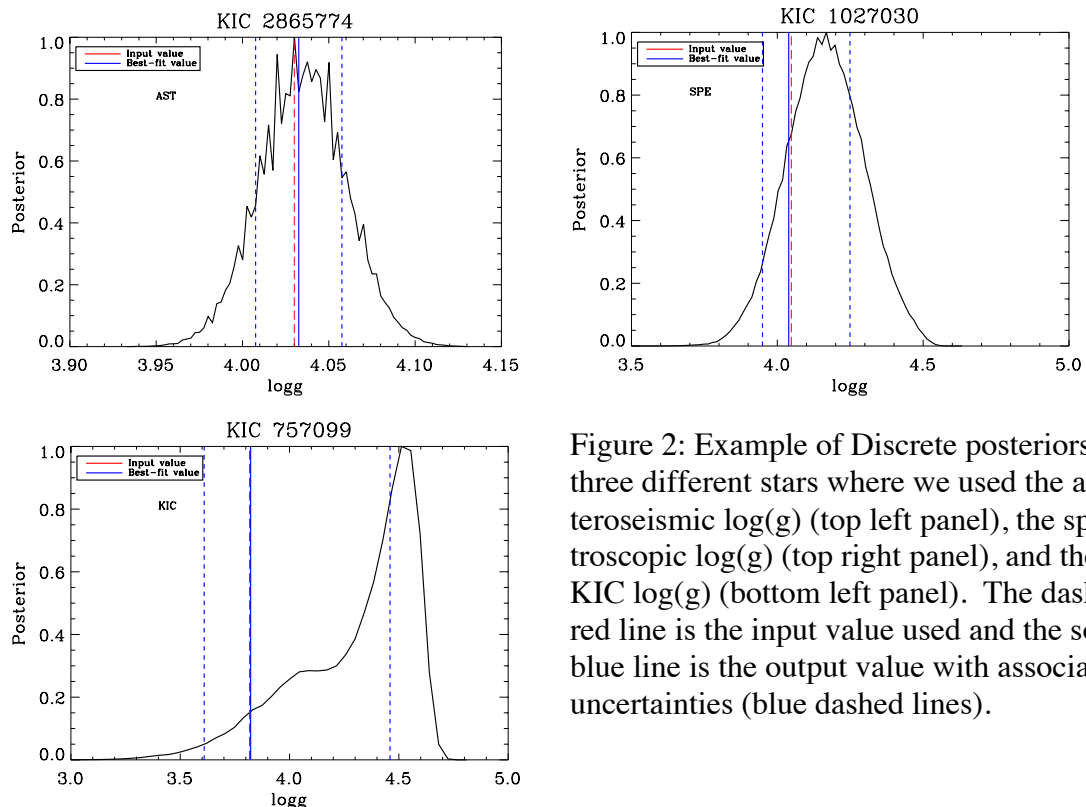

Figure 2: Example of Discrete posteriors for three different stars where we used the asteroseismic log(g) (top left panel), the spectroscopic log(g) (top right panel), and the KIC log(g) (bottom left panel). The dashed red line is the input value used and the solid blue line is the output value with associated uncertainties (blue dashed lines).

For stars with input values that fall off the Dartmouth grid (*e.g.*, very cool dwarfs) we adopted the input and output values from Huber et al. (2014). There are also three stars where we adopted published literature values for all stellar parameters (*i.e.*, KIC 5807616, 5868793 and 10001893). Indeed these three stars fall out of the grid because they are too hot with temperatures above 25,000K. Unlike previous deliveries, we did not override catalog values with published solutions that provide better estimates for radii and masses (*e.g.*, from asteroseismology) in order to homogeneously derive posterior distributions (including distances) for all stars. This means that for some stars better estimates for radius and mass may be available in the literature. We also emphasize that the DSEP isochrones do not include He-core burning models, and hence systematic errors in stellar properties (in particular masses) for red giants should be expected (see Huber et al. 2014 for details) compared to more detailed studies (*e.g.*, Pinsonneault et al. 2014).

The new catalog also includes several corrections that were pointed out by the community since the release of the Q1-Q16 catalog. Due to a coding error, every star in the Q1-Q16 catalog with input $T_{eff} < 3250K$ was automatically classified as a dwarf using BT-Settl models even if the input T_{eff} indicated that it was a giant. To correct this, we revisited all dwarfs that were classified using BT-Settl models and verified their evolutionary state using the Mann et al. (2012) spectroscopic classifications. When this was verified, we adopted the Q1-Q16 BT-Settl solution.

The reported uncertainties are the one-sigma values associated with the best-fit values. We note that the uncertainties are somewhat smaller than in the previous catalog due to the volume weighting of each isochrone point, which was not taken into account in the Q1-Q16 catalog.

For this delivery, two additional outputs are provided: distances and the extinction in the V-band (Av). To compute the distance, we take the J-band magnitude when available or the g-band, and calculate a distance using absolute magnitudes from the Dartmouth grid and the 3D reddening model of Amores & Lepine (2005). We adopt the reddening law from Cardelli et al. (1989) with $A_V/A_J=1.234$ and $A_V/A_g=0.288$.

2.3 Output Quantities

The outputs delivered in this catalog are best fit values and one-sigma confidence intervals for mass, radius, surface gravity, effective temperature, density, metallicity, distance and Av. Figure 3 represents the HR diagram of the output from the Q1-Q17 DR24 catalog (previous delivery, right panel) and the Q1-Q17 DR25 catalog (this delivery, left panel). We clearly see a larger "eye" around the main sequence/subgiants area in the current delivery. This means that we have more subgiants than before, which is mostly due to the LAMOST and Flicker results.
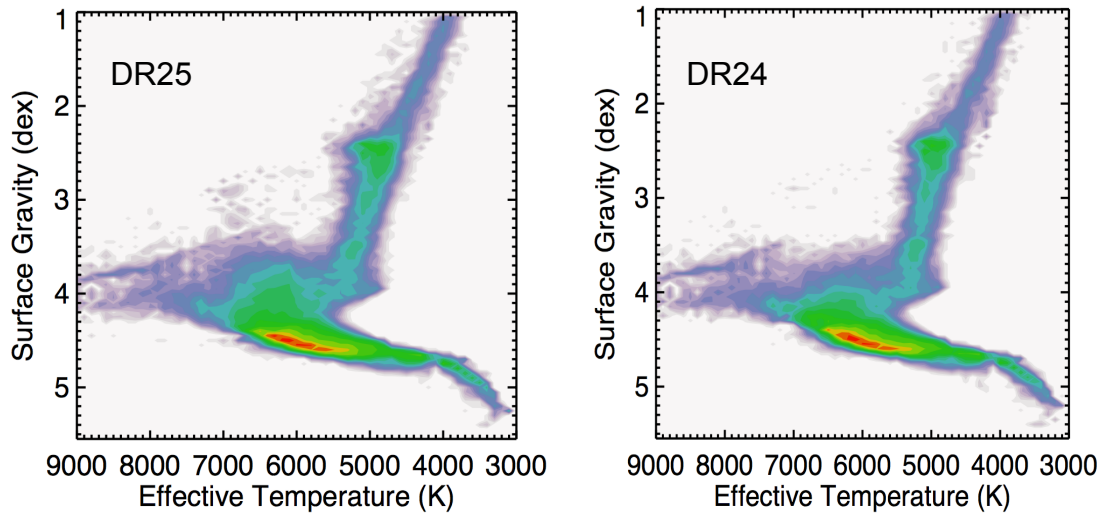
Figure 3: Output values of the new delivery (Q1-Q17 DR25, left panel) and the previous delivery (Q1-Q17 DR 24, right panel). Color denotes number density of stars as in Huber et al. (2014).

Figure 4 shows the distance distribution for *Kepler*-observed dwarfs with $T_{eff} < 6700K$ and $\log(g) > 3.5$ (left panel) and for red giants with $T_{eff} < 5000K$ and $\log(g) < 3.5$ (right panel). As expected, the red giants are much more distant than dwarfs.
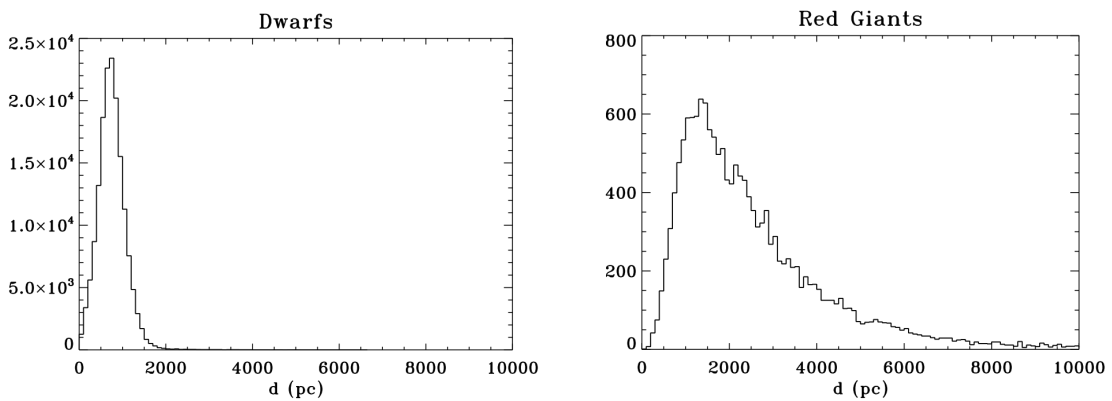

Figure 4: Distribution of distances for dwarfs (left panel) and red giants (right panel) in the new catalog delivery.

2.4 Comparison of Planet-Candidate Host Star Parameters

Figure 5 compares DSEP radii and masses of the planet host stars between the current delivery and the previous Q1-Q17 DR24 catalog.

It is comforting to see that stars with the same inputs as before (*i.e.*, the black diamonds in the figure) fall on or very close to the line $R_{Q1-Q17}/R_{new}=1$, so these stars change by a few percent at most. Such small changes are explainable by the new methodology that has been applied (best-fit value instead of the median) and the updated grid where we have filled some existing gaps.

Not surprisingly, the largest changes are found for stars with new input data.

1) Many stars with new CFOP parameters have a different evolutionary stage. Indeed, we mentioned earlier that a fraction of the stars moved from the main sequence to become more evolved subgiants. This explains the number of stars (cyan symbols) that have a larger radius than in the previous catalog. This is also the case for the star with Flicker input (blue symbol) and some of the individual new inputs (pink symbols).

2) For the stars cooler than ~4500K, we notice that many become smaller and less massive. We believe that in many cases the new spectroscopic observations for these cool stars led to a higher $\log(g)$, and thus a smaller radius. In addition to the change of the input value, the new updated grid contributed to these changes in the stellar parameters as well.

Some particular cases of outliers:

1) Two stars, KIC 5640085 (KOI-448) and KIC 10027323 (KOI-1596), with T_{eff} around 4000K and R_{Q1-Q17}/R_{new}~1.4-1.5, were using inputs from SPE58 but were actually too hot and too large in the Q1-Q17 DR24 catalog. The input parameters were reversed back to the Q1-Q16 catalog as SPE5.

2) KIC 7529266 (KOI-680) has the largest change in radius (R_{Q1-Q17}/R_{new}~0.3) due to updated input values from SPE76, which yields a $\log(g)$ of 3.5 (*i.e.*, a subgiant) compared to the $\log(g) = 4.35$ dwarf classification in the KIC.

3) The decrease in radius for KIC 8733898 (KOI-2842, R_{Q1-Q17}/R_{new}~1.4) is due to a significantly cooler spectroscopic temperature (SPE86) compared to the previous photometric classification (PHO2).

4) Finally, KIC 7582689 (KOI-3097) is a solar-type star with a significantly decreased radius. It has a larger $\log(g)$ input value from SPE84 (of 4.40 dex) compared to the previous catalog (of 4.13 dex) and thus a smaller radius.
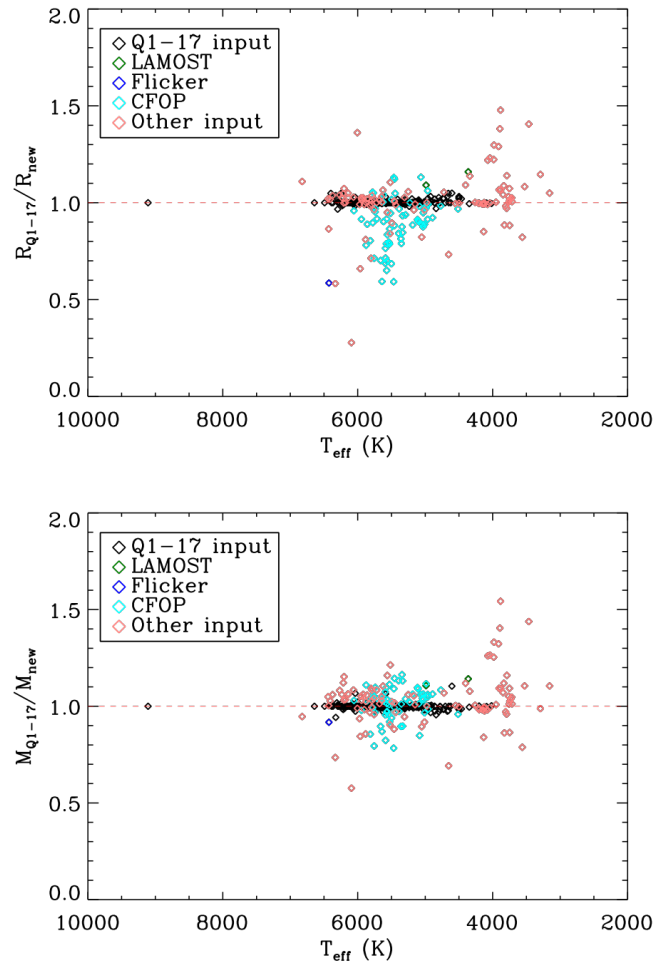
Figure 5: Comparison of the radii and masses of the planet host stars showing the different subsamples where we used either new or the same input values as in the previous catalog.

3.   Stellar Replicated Posterior Samples

In the remainder of this document, we use the following terminology to refer to different types of posteriors:

- MCMC posteriors: posteriors obtained from traditional MCMC chains

- Discrete posteriors: discrete posterior probability distribution functions obtained following Serenelli et al. (2013) by directly integrating isochrones given input constraints

- Replicated posteriors: posteriors delivered here that are approximations of the Discrete posteriors constructed as described hereafter.

Replicated posteriors for all stellar parameters are provided for each target in the catalog where we applied the Serenelli et al. (2013) method. We note that these are not MCMC posteriors but approximations of Discrete posteriors.

The method for approximating a Discrete posterior is as follows. The Discrete posteriors are based on a subset of ~400,000 models from the grid of models used. Each model is a point on the isochrones and is described by a set of star parameters (*i.e.*, T_{eff}, [Fe/H], log g, M, R, *etc*.). From the Discrete posterior, each individual model has some probability x. We scale the Discrete posterior by a factor N_scale so that the Discrete posterior now goes from 0 to N_scale. After a few tests N_scale was fixed to 50. Then we draw a random model (from a uniformly random process) with a probability x from the Discrete posterior and replicate all its parameters x*N_scale times. If x*N_scale<1, the model is not replicated. The drawing is repeated until the number of samples reaches the total number of samples desired, N_sample, which for this delivery was fixed at 40,000. This value for N_sample was chosen as a compromise between achieving appropriate correlation lengths and keeping the file sizes to a reasonable value for each star. A histogram of the Replicated posteriors provides the approximation of the Discrete posteriors, which are binned versions of the individual model probabilities along a given parameter. Importantly, the Replicated posteriors conserve correlations between the parameters because each set is drawn so as to correspond to a self-consistent model.

Figure 6 shows a comparison between the stellar Replicated Posterior samples obtained for Kepler-452 (Jenkins et al. 2015), and the classical MCMC posteriors for the three parameters T_{eff}, M, and R. Both methods give similar distributions, validating the approximation method yielding the Replicated posteriors.
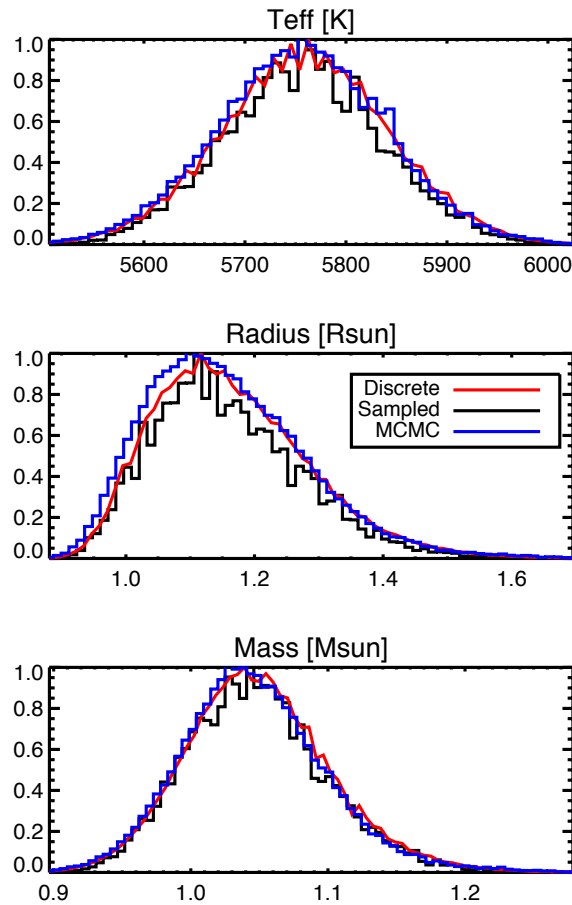
Figure 6: Comparison between the MCMC posteriors (blue line) and the Replicated posteriors (black line) obtained from the method applied in this delivery for the Kepler planet-host star, Kepler-452.

Figure 7 shows an example comparison between Discrete posteriors and the Replicated posteriors constructed as explained above for a dwarf (KIC 757076). The Replicated posteriors show good agreement with the Discrete posteriors. We checked the results for different spectral types and they looked similar to this example.

We provide in the files the distribution of the different parameters as well as the logarithm of the likelihood as computed in Huber et al. (2014) and the logarithm of the weight, which is the volume of the model in mass, metallicity, and age. The priors are not listed as we used flat priors on these quantities.

Finally, we remind the reader that the Replicated posteriors are provided for 196,850 stars as ~250 stars fall of the grid. These are either very cool dwarfs (T_{eff} < 3250 K or hot stars wih T_{eff}>25000K) and we used other solutions for them so they have null uncertainties.
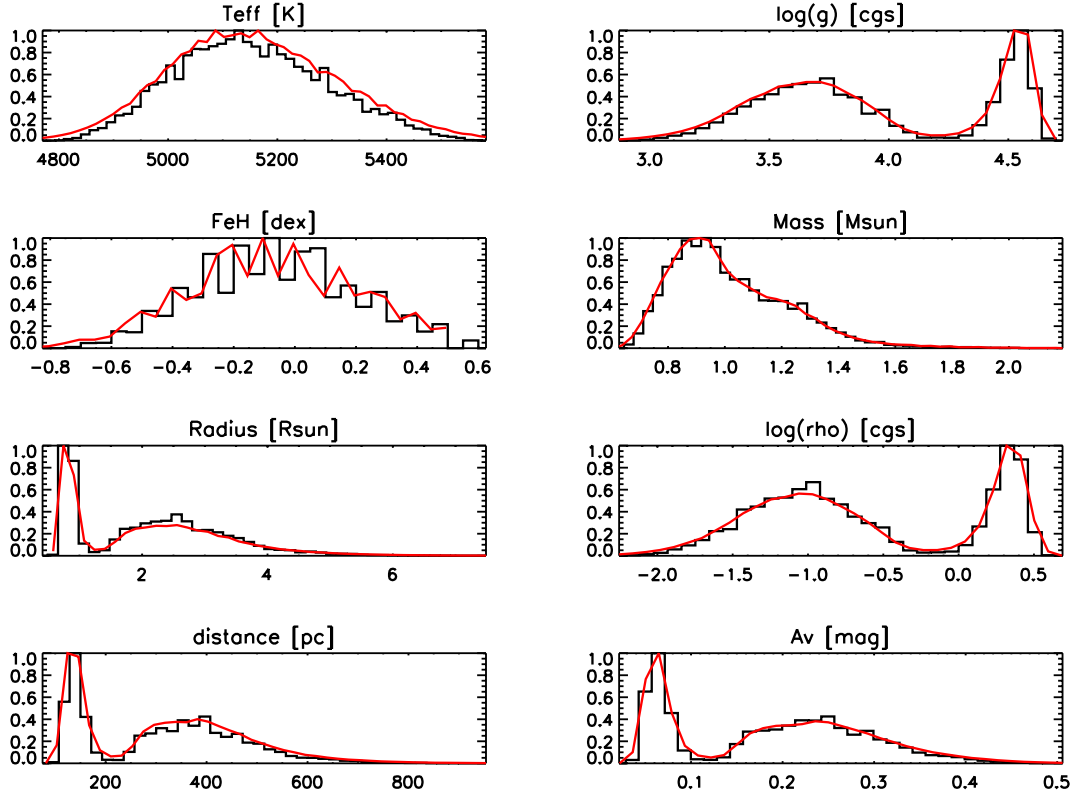

Figure 7: Example of Discrete posteriors (red lines) with the Replicated posteriors built as described in the text (black lines).

Worked examples:

We show here some simple examples on how to use these Replicated posteriors files. They have the generic name: *kplr<kepler_id>_dr25-stellarposterior.txt'* and contain 10 space-separated columns for each star:

Teff, Logg, Fe/H, Mass, Radius, log(rho), distance, Av, log(likelihood), log(weights).

The weights are computed as described above, following Serenelli et al. (2013). We note that we have assumed flat priors in age, metallicity, and mass in our analysis, and hence these are not listed separately.

Commands in IDL:

```
;Example 1.  Generating the plots shown in Figure 8.  The plots
in Figure 9 only require a change in input file name.

;Reading the file for a single star:

> readcol, 'kplr008073672_dr25-stellarposterior.txt', teff, logg,
feh, M, R, rho, d, Av, lh, weights

;Plotting the correlation between Teff and Radius:

> plot, teff, R, psym=7, xtit='Teff (K)', ytit='R (Rs)'

;Plotting the correlation between Mass and Radius:

> plot, M, R, psym=7, xtit='M (Ms)', ytit='R (Rs)'

;Plotting the correlation between log(g) and distance:

> plot, logg, d, psym=7, xtit='log g', ytit='d (pc)'
```
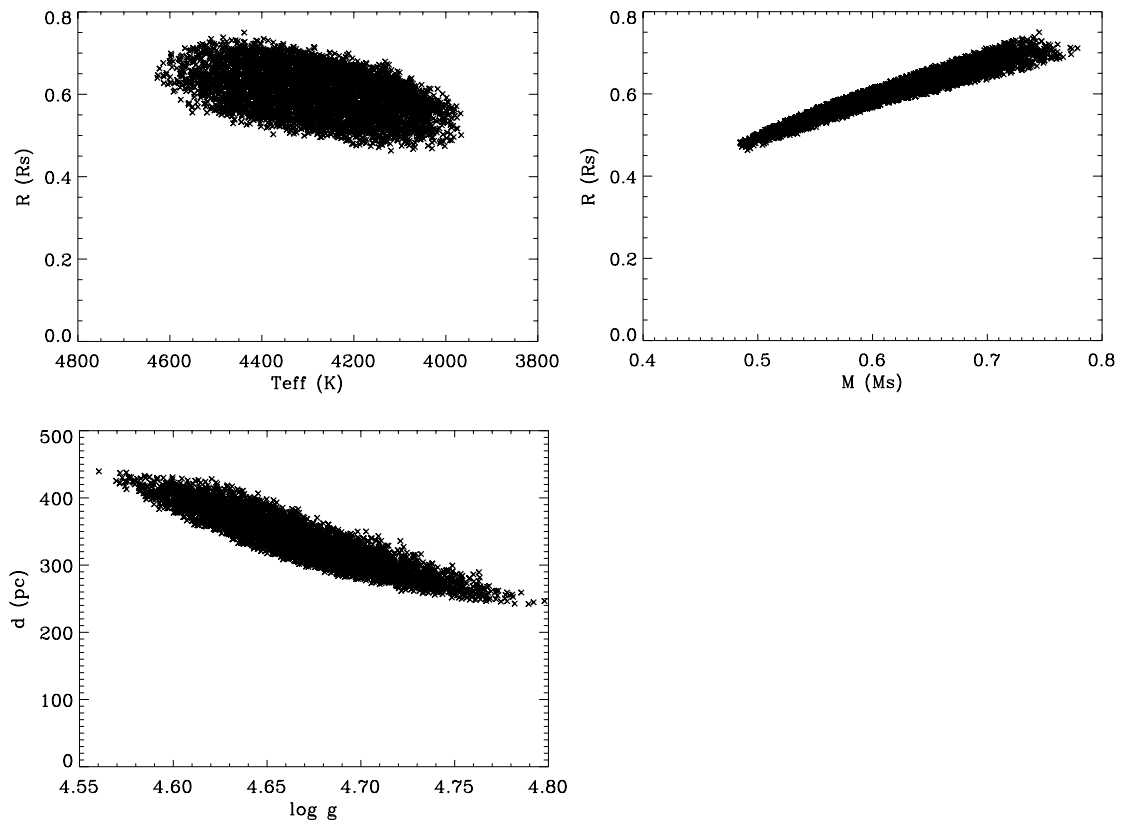

Figure 8: Example correlation plots for the cool dwarf KIC 8073672.
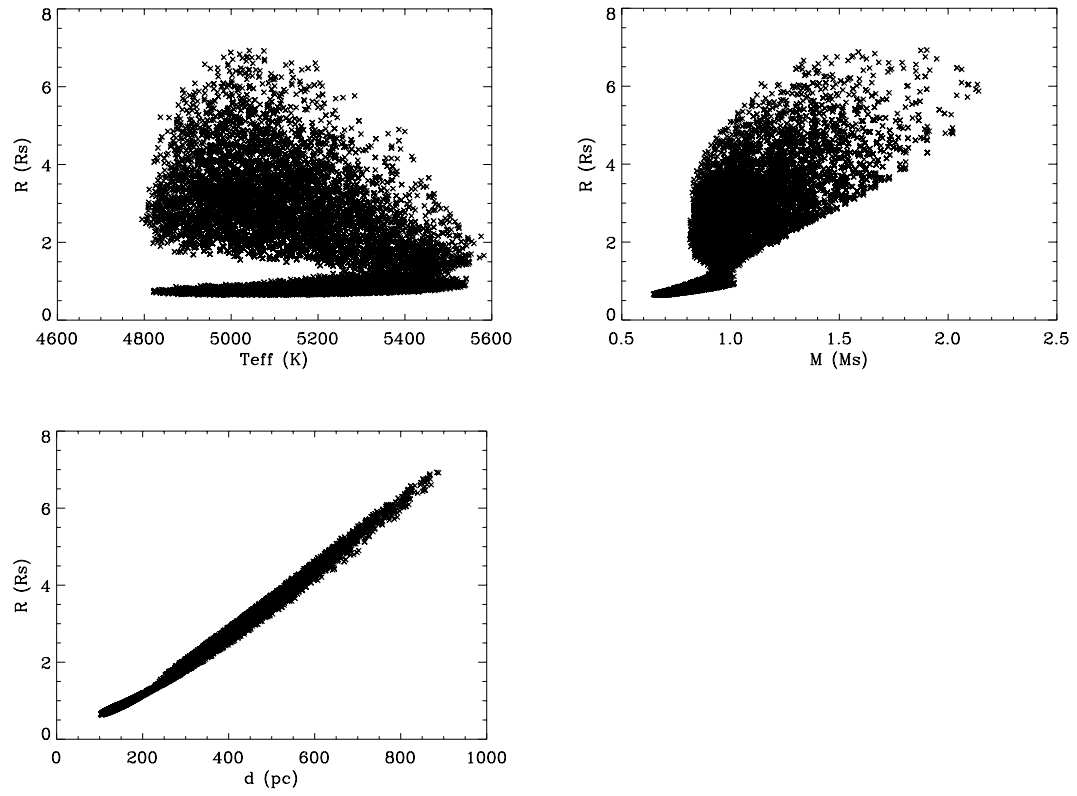
Figure 9: Example correlation plots for the cool dwarf KIC 757076.

```
;Example 2.  Generating the plots shown in Figure 10.

;Reading the file for a single star:

> readcol, 'kplr000757076_dr25-stellarposterior.txt', teff, logg,
feh, M, R, rho, d, Av, lh, weights

;Plotting histograms of results:

> plothist, Teff, bin=10, peak=1, xtit='Teff (K)'

> plothist, M, bin=0.05, peak=1, xtit='M (Ms)'
```
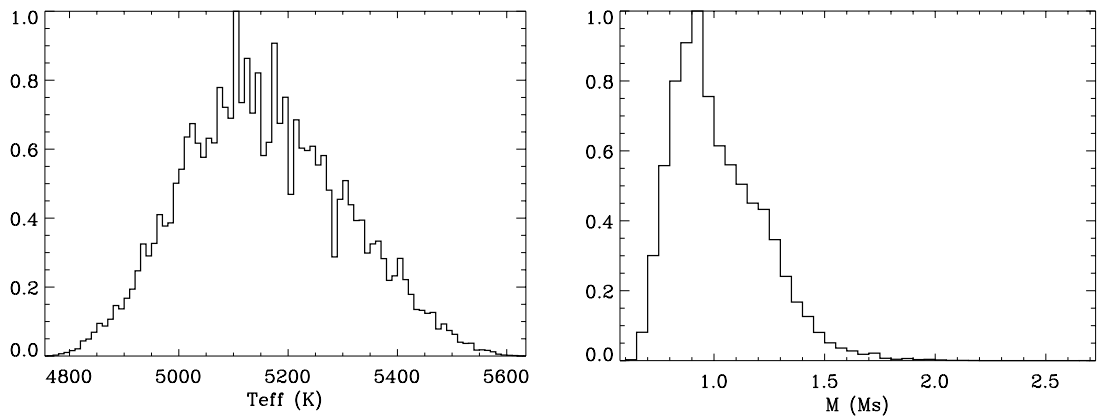

Figure 10: Example histograms for the stellar Replicated posteriors of KIC 757076.

```
;Example 3.  Reducing the number of samples

> Teff_s=dblarr(4e3)

> n=10 ; take 1 point out of 10

> for i=0, n_elements(Teff_s)-1 do Teff_s(i)=Teff1(n*i)
```

4.   Updated Distances and Extinction Values (ERRATUM)

Due to a coding error in the isochrones fitting code, the extinction values in the J-band and g-band were swapped in the previous delivery dated April 15, 2016, leading to incorrect distances and extinction values. Since most distances were derived from *J*-band, this resulted in a systematic underestimation of reported distances by an average of ~20% for typical solar-type stars, and up to ~50% for more distant red giant stars. Correspondingly, this also led to a systematic overestimation of A_V values by up to ~0.05 mag.

The corrected values will be live at NASA's Exoplanet Archive on or about November 10, 2016. Any distances and extinction values downloaded before this date should not be used. Similarly, the replicated posteriors (see Section 5) for these erroneous distances and extinction values should not be used. Revised values are currently being computed and will be available through the Archive starting in December, 2016.

5. Summary

The *Kepler* Q1-Q17 DR25 stellar properties catalog includes improved stellar properties for 28,800 stars including spectroscopic inputs from surveys (CFOP, APOGEE, LAMOST), the Flicker log(g), and the reclassification of more than 800 stars. We also added 310 stars that were first observed during the last *Kepler* quarter, Q17. Finally, 317 stars that were unclassified because they lacked reliable 2MASS colors now have spectroscopic parameters from LAMOST and APOGEE. This increases the total number of stars in the *Kepler* catalog to 197,096, including 4085 planet(-candidate) host stars.

This Q1-Q17 DR25 star properties catalog was used for the Q1-Q17 DR25 TPS/DV planet search. This catalog and the associated stellar replicated posteriors (see Section 3) are available at the NASA Exoplanet Archive: http://exoplanetarchive.ipac.caltech.edu.

6.   References

Amores, E. B., & Lepine, J. R. D, 2005, AJ, 130, 659

Alam, S., et al. 2015, ApJS, 219, 12

Almenara, J. M., et al. 2015, A&A, 575, 71

Bastien, F., et al. 2013, Nature, 500, 427

Bastien, F., et al. 2014, ApJ, 788, 9

Bastien, F., et al. 2015, submitted to ApJ

Batalha, N., et al. 2010, ApJ, 713, L109

Borucki, W. J., et al. 2012, ApJ, 745, 120

Borucki, W. J., et al. 2013, Science, 340, 587

Bourrier, V., et al. 2015, A&A, 579, 55

Buchhave, L. A., et al. 2014, Nature, 509, 593

Cardelli, J. A., et al. 1989, ApJ, 345, 245

Casagrande, L., et al. 2014, ApJ, 787, 110

Dawson, R. I., et al. 2014, ApJ, 791, 89

Deleuil, M., et al. 2014, A&A, 564, A56

Dotter, A., Chaboyer, B., Jevremovic, D., Kostov, V., Baron, E., & Ferguson, J. W. 2008, ApJS, 178, 89

Endl, M., et al. 2014, ApJ, 795, 151

Everett, M. E., et al. 2015, AJ, 149, 55

Gandolfi, D., et al. 2013, A&A, 557, A74

Gandolfi, D., et al. 2015, A&A, 576, 11

Hébrard, G., et al. 2014, A&A, 572, 93

Huber, D., et al. 2014, ApJS, 211, 2

Jenkins, J., et al. 2015, AJ, 150, 56

Kipping, D. M., et al. 2014, ApJ, 795, 25

Lillo-Box, J., et al. 2015, A&A, 577, 105

Luo, A-Li, et al. 2015, RRA, 15, 1095

Mancini, L., et al. 2015, arXiv1504.04625

Maan, A. W., et al. 2012, ApJ, 753, 90

Mann, A. W., Gaidos, E., & Ansdell, M. 2013a, ApJ, 779, 188

Mann, A. W., Gaidos, E., Kraus, A., & Hilton, E. J. 2013b, ApJ, 770, 43

Marcy, G. W., et al. 2014, ApJS, 210, 20

Muirhead, P. S., et al. 2014, ApJS, 213, 5

Muirhead, P. S., et al. 2015, ApJ, 801, 18

Ofir, A., Dreizler, S., Zechmeister, M., & Husser, T.-O. 2014, A&A, 561, A103

Petigura, E. A., Howard, A. W., & Marcy, G. W. 2013, PNAS, 110, 19175

Pinsonneault, M. H., et al. 2014, ApJS 215, 19

Rowe, J. F., et al. 2014, ApJ, 784, 45

Sanchis-Ojeda, R., et al. 2013, ApJ, 775, 54

Santerne, A., et al. 2014, A&A, 571, 37

Seader, S., et al. 2015, ApJS, 217, 18

Serenelli, A., et al. 2013, MNRAS, 429, 3645

Silva Aguirre, V., et al. 2015, MNRAS, 452, 2127

Silvotti, R., et al. 2014, A&A, 570, 130

Tenenbaum, P., et al. 2014, ApJS, 211, 6

Tingley, B., et al. 2014, A&A, 567, A14

Torres, G., et al. 2015, ApJ, 800, 99

Twicken, J., et al. 2016, arXiv:1604.06140